nature chemistry

ARTICLES

PUBLISHED ONLINE: 12 DECEMBER 2016 | DOI: 10.1038/NCHEM.2670

An iron-catalysed C–C bond-forming spirocyclization cascade providing sustainable access to new 3D heterocyclic frameworks

Kirsty Adams[1], Anthony K. Ball[1], James Birkett[1], Lee Brown[1], Ben Chappell[2†], Duncan M. Gill[1], P. K. Tony Lo[1], Nathan J. Patmore[1], Craig. R. Rice[1], James Ryan[1], Piotr Raubo[2,3] and Joseph B. Sweeney[1]*

Heterocyclic architectures offer powerful creative possibilities to a range of chemistry end-users. This is particularly true of heterocycles containing a high proportion of sp^3-carbon atoms, which confer precise spatial definition upon chemical probes, drug substances, chiral monomers and the like. Nonetheless, simple catalytic routes to new heterocyclic cores are infrequently reported, and methods making use of biomass-accessible starting materials are also rare. Here, we demonstrate a new method allowing rapid entry to spirocyclic bis-heterocycles, in which inexpensive iron(III) catalysts mediate a highly stereoselective C–C bond-forming cyclization cascade reaction using (2-halo)aryl ethers and amines constructed using feedstock chemicals readily available from plant sources. $Fe(acac)_3$ mediates the deiodinative cyclization of (2-halo)aryloxy furfuranyl ethers, followed by capture of the intermediate metal species by Grignard reagents, to deliver spirocycles containing two asymmetric centres. The reactions offer potential entry to key structural motifs present in bioactive natural products.

Metal-catalysed C–C bond-forming reactions have revolutionized contemporary synthetic chemistry in academia and industry, and commercial products (including polymers, diagnostic materials, fine chemicals and active drug substances) are regularly prepared in bulk using these methods. Modern catalysis researchers are faced with additional financial, regulatory and environmental demands to deliver lower waste-footprints, as well as more efficient and cost-effective methods for catalytic C–C bond formation; these demands have stimulated intense interest in the use of Earth-abundant catalysts[1–3] and recently the application of iron catalysts in particular has received much attention[4–7]. In parallel, the use of biomass to deliver high-value chemical commodities has been recognized as increasingly significant when traditional sources for chemical feedstocks dwindle. The application of catalysis to encompass biomass-derived substrates is, therefore, an impactful research theme.

Chemical processes delivering functional heterocycles are also inherently impactful, due to the known utility of these small molecules. Within the broad heterocyclic sub-class, the presence of heteroatoms constrained about quaternary carbon centres endows well-defined spatial constraints that are often beneficial, for instance in enhancing selectivity in drug-binding. Within this sub-class, heterocycles bearing quaternary centres are privileged molecules[8]; 1,7-bis-heterospirocycles (Fig. 1a) are members of this family of constrained small molecules, with both natural (such as genkwanol A (ref. 9) and aspergillines (ref. 10)) and synthetic examples (such as BRD7016 (refs 11,12) and compound **1** (ref. 13)) of these structures reported to be bioactive. However, synthetic access to the core framework of this class of spirocycle is limited. The practical preparative routes that allow access to the ring systems shown in Fig. 1 most often feature [2+3] cycloadditions (Fig. 1b). This reaction class most often features tandem formation of C–C and C–X bonds, often in two distinct steps[14].

We hypothesized that spiroheterocycles could be accessed efficiently via an iron-catalysed C–C bond-forming cascade (Fig. 1c), involving a tandem cyclization–alkylation process. We predicted that an aryl-iron species **2** (formed by insertion into a halide or pseudohalide bond of the iron complex created by reaction of an iron(III) salt with a Grignard reagent) would undergo dearomatizing cyclization[15] onto a pendant furan scaffold, followed by reductive elimination of the most stable allyl-iron isomer (**3**) to give alkyl- or arylated product **4**. In addition to allowing an innovative entry to the spirocyclic motif, the incorporation of an alkene in the product also allows for further diversification and mapping of chemical space. Here we report the realization of this strategy, and the delivery of a novel and sustainable iron(III)-catalysed arylative spirocyclization reaction which delivers spiro bis-heterocycles efficiently and stereoselectively.

Results

A core feature of our strategy (Fig. 1c) was the use of substrates that could be derived in bulk from biomass, offering the prospect of a more sustainable method for accessing novel spiro heterocycles. Thus we targeted the use of furfuryl alcohol as a lynchpin biomass-derived component, available in bulk directly from plant sources (such as corn cobs[16]) using simple benchtop procedures. Activation followed by reaction with 2-halophenols gave the cyclization templates **5**-Hal (Table 1), which were reacted with phenyl magnesium bromide at room temperature in the presence of $Fe(acac)_3$ (5 mol %). Though reaction with the chloride was not productive[17], the corresponding bromide and iodide delivered phenylated spirocycle **6a** directly (Table 1, entries 2 and 3).

The tricyclic product **6a** was delivered from the reaction of iodoether **5-I** as an 85:15 ratio of diastereoisomers (deduced from

[1]Department of Chemical Sciences, University of Huddersfield, Huddersfield HD1 3DH, UK. [2]AstraZeneca Pharmaceuticals, Alderley Park, Macclesfield SK10 4TG, UK. [3]AstraZeneca Pharmaceuticals, Oncology Chemistry, Hodgkin Building, c/o Darwin Building, Unit 310, Cambridge Science Park, Milton Road, Cambridge CB4 0FZ, UK. †Present address: Department of Chemistry, University of Cambridge, Lensfield Road, Cambridge CB2 1EW, UK.
*e-mail: j.b.sweeney@hud.ac.uk

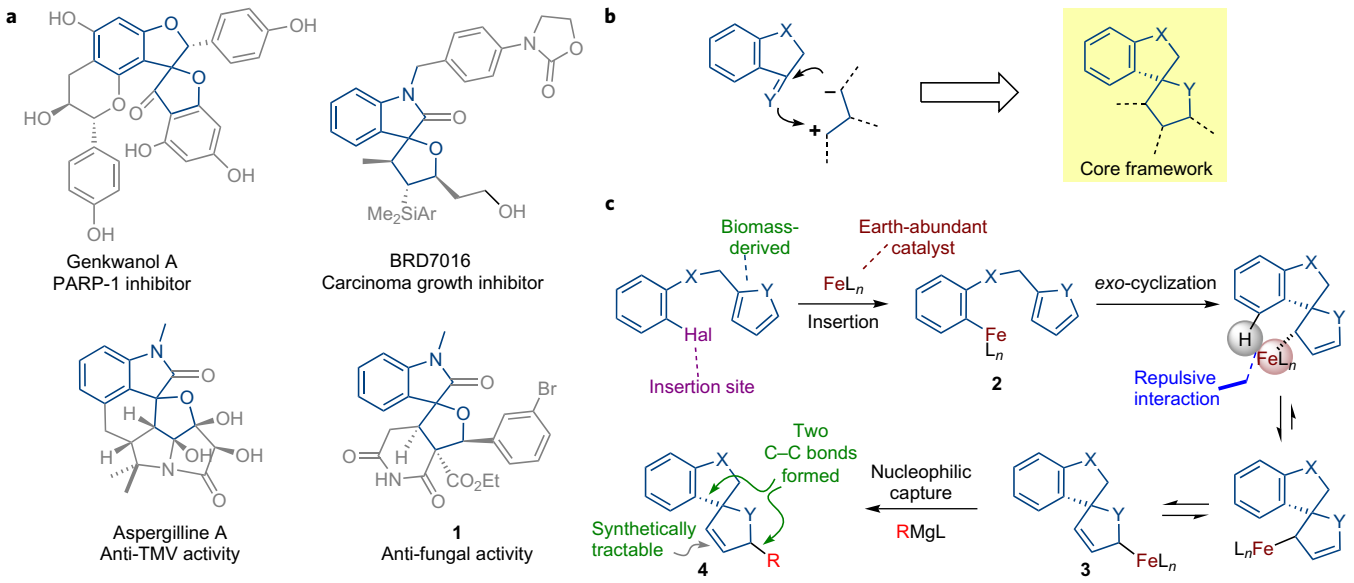

Figure 1 | Synthesis of spirocyclic bis-heterocycles that are the cores of natural products. a, Selected examples of biologically active natural products featuring spirocyclic bis-heterocycles. The activity and biological properties of these molecules are often heavily predicated on the 3D arrangement of the heteroatoms at their cores. Spirocycles result in a unique spatial arrangement of these heteroatoms and play a key role in binding to biomolecules. **b**, The [2+3] cycloaddition is the most frequently used method used to access spirocyclic bis-heterocycles. However, this approach places limitations on the substrates that can be used as precursors to spirocycles, sometimes requiring tailored electronic properties for the coupling partners. **c**, This work demonstrates a new strategy for preparing spirocyclic bis-heterocycles using an iron-catalysed cyclization/nucleophile-capture process. In addition to using an inexpensive Earth-abundant catalyst, this approach broadens the scope of suitable substrates and permits the inclusion of an alkene in the ultimate product, which can be used for further elaboration.

Table 1 | Influence of solvent, catalyst and stoichiometry on iron-catalysed cascade.

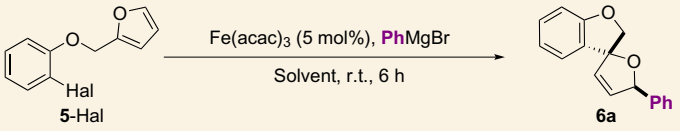

Entry	Catalyst	5-Hal	Solvent	PhMgBr eq.	Conversion (%)	Yield 6a (%)
1	$Fe(acac)_3$	5-Cl	THF/NMP (8:1)	1.2	100	0
2	$Fe(acac)_3$	5-Br	THF/NMP (8:1)	1.2	100	29
3	$Fe(acac)_3$	5-I	THF/NMP (8:1)	1.2	100	41
4	$Fe(acac)_3$	5-I	NMP	1.2	100	9
5	$Fe(acac)_3$	5-I	THF/NMP (1:3)	1.2	100	36
6	$Fe(acac)_3$	5-I	THF/NMP (1:1)	1.2	100	44
7	$Fe(acac)_3$	5-I	THF/NMP (3:1)	1.2	100	27
8	$Fe(acac)_3$	5-I	THF	1.2	100	30
9	$Fe(acac)_3$	5-I	Et_2O/NMP (8:1)	1.2	100	33
10	$Fe(acac)_3$	5-I	NMP	1.2	100	27
11	$Fe(acac)_3$	5-I	Et_2O/NMP (1:3)	1.2	100	37
12	$Fe(acac)_3$	5-I	Et_2O/NMP (1:1)	1.2	100	55
13	$Fe(acac)_3$	5-I	Et_2O/NMP (3:1)	1.2	100	27
14	$Fe(acac)_3$	5-I	Et_2O	1.2	100	19
15	$Fe(acac)_3$	5-I	DMF/NMP (8:1)	1.2	100	0
16	$Fe(acac)_3$	5-I	DMPU/NMP (8:1)	1.2	100	0
17	$Fe(acac)_3$	5-I	DMA/NMP (8:1)	1.2	100	12
18	$Fe(acac)_3$	5-I	Dioxane/NMP (8:1)	1.2	100	0
19	-	5-I	Et_2O/NMP (1:1)	1.2	0	0
20	$Fe(acac)_3$	5-I	Et_2O/NMP (1:1)	-	0	0
21	$Fe(acac)_3$	5-I	Et_2O/NMP (1:1)	1.2	100	63
22	$Fe(acac)_3$	5-I	Et_2O/NMP (1:1)	1.8	100	64
23	$Fe(acac)_3$	5-I	Et_2O/NMP (1:1)	2.4	100	73
24	$FeCl_3$	5-I	Et_2O/NMP (1:1)	2.4	100	70
25	$Fe(dbm)_3$	5-I	Et_2O/NMP (1:1)	2.4	43	7
26	$Fe(dpm)_3$	5-I	Et_2O/NMP (1:1)	2.4	100	39
27	$Fe_2(SO_4)_3$	5-I	Et_2O/NMP (1:1)	2.4	0	0

dbm, dibenzoylmethide; dpm, dipivaloylmethide; NMP, N-Methyl-2-pyrrolidone.

Table 2 | Scope of Grignard partner in iron-catalysed arylative spirocyclization.

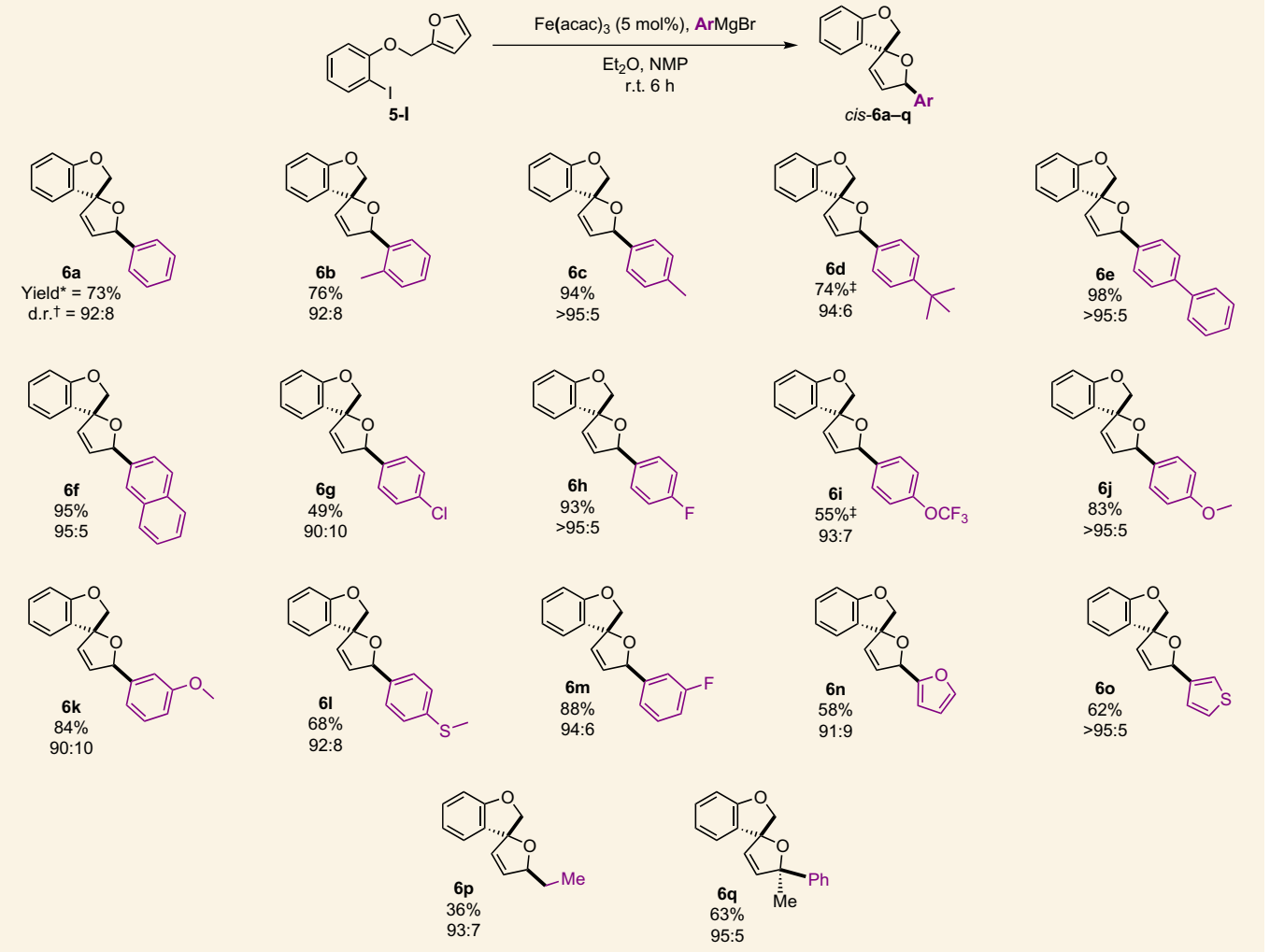

*Isolated yield of major diastereomer; †Determined by HPLC analysis of crude product; ‡Catalyst = $FeCl_3$.

^{1}H NMR experiments), in favour of the *cis*-spirocycle in which the two new C–C bonds are formed on opposite sides of the dihydrofuran motif. Armed with these most encouraging preliminary data, we proceeded to the optimization phase of the project. Being mindful of Cahiez's seminal studies[18] of the interplay of solvent and additives in iron-catalysed C–C bond-forming reactions, we looked at the effect of solvent on the reaction, with additional focus on the relative NMP content (Table 1). This screening process indicated the optimum reaction medium to be Et_2O/NMP (1:1, Table 1, entry 12).

The next phase of optimization examined a range of stable iron(III) catalysts in the arylative spirocyclization reaction (Table 1, entries 23–27). It was confirmed that the catalyst was essential for the reaction to take place (entry 19) and that $FeCl_3$ seemed generally as effective a catalyst as $Fe(acac)_3$ (entry 24). When Grignard reagent was omitted, starting material was returned. It was notable that conversion and yields were consistently improved when an excess of Grignard reagents was employed, with the use of 2.4 equivalents leading to the highest yields. Iron complexes bearing bulkier ligands were less productive in the reaction (entries 25 and 26) but only $Fe_2(SO_4)_3$ proved ineffective, resulting in no conversion (entry 27). Having identified an optimized reaction protocol (Table 1, entry 23), we turned to an examination of the scope of the reaction.

It quickly transpired that this arylative spirocyclization reaction is highly stereoselective, generally efficient using a range of aryl and heteroaryl Grignards (Table 2), delivering previously unknown spiroheterocycles as predominantly *cis*-diastereomers (confirmed by X-ray analysis of product **6c**, Supplementary page 45). Though the reaction of aryl Grignards was productive, in accord with previous observations the use of alkyl Grignard reagents in the spirocyclization reaction was not efficient, with only EtMgBr delivering alkylated product **6p** (Table 2) in reasonable quantities.

One of the attractive features of iron-catalysed organometallic reactions is the decreased tendency for termination via β-hydride elimination of C–Fe σ-bonds. Since the postulated intermediates in the reaction described above did not have the possibility for reductive elimination, we were keen to test a substrate where reductive elimination was possible, such as 5′-methyl substrate (easily accessible from furfuryl alcohol[19]); when this compound was used in the arylative spirocyclization reaction, a good yield of arylated product **6q** was obtained (Table 2), confirming the low propensity of the intermediate iron species to undergo reductive elimination.

The ability to incorporate other substituents into the aromatic ring of the substrate, and the ability to deliver nitrogen-containing heterocycles using this method were important requirements for the process. Thus we were delighted to observe that the iron-catalysed arylating spirocyclization reaction does indeed allow access to a range of nitrogen-containing heterocycles, and also products

Table 3 | Scope in heteroatom and substituent pattern in iron(III)-catalysed arylative spirocyclization.

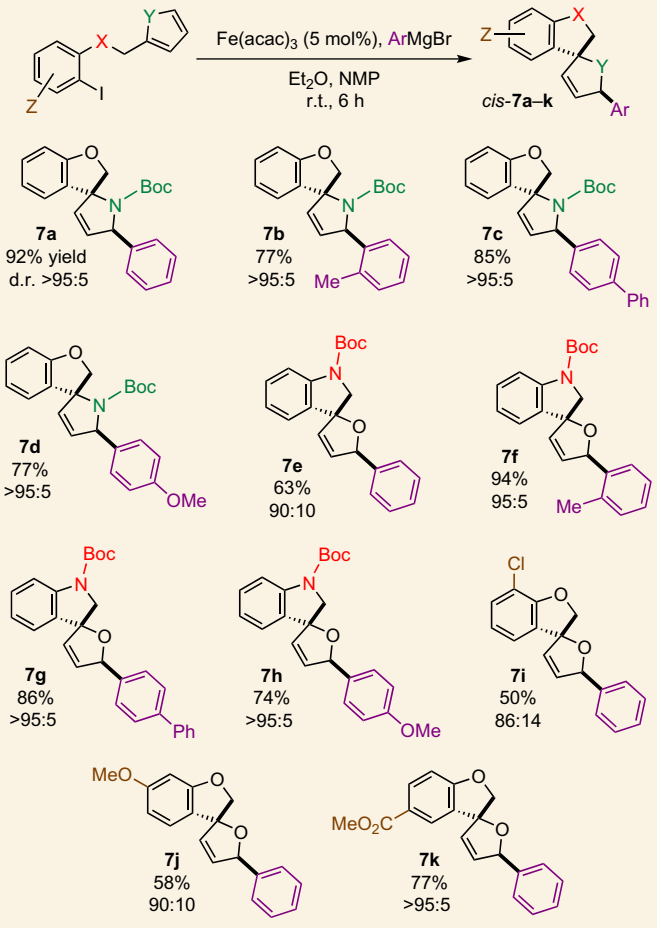

bearing substituents in the parent carboaromatic ring (Table 3). Of particular note are products **7i** and **7k**, containing potentially fragile halogen and ester moieties, respectively.

Discussion

Having demonstrated the power of our new method in the preparation of novel, natural-product-like spiroheterocycles, we turned our attention to the mechanistic features of the reaction.

The mechanisms in play during iron-catalysed cross-coupling reactions[20,21] are complex and often not well-understood, and the dearomatizing arylative spirocyclization described here could involve one of several possible pathways. We believe that it is likely that the reaction proceeds via a catalytically competent Fe(II) species[22–25] leading to σ-aryl iron intermediate **8** which cyclizes to give η^1-allyl iron species **9** (Fig. 2), able to equilibrate[26] to η^3-isomer **10**. If **10** is able undergo isomerization (by dissociation–recomplexation or homolysis–recombination) to avoid a repulsive *peri* interaction, it will be converted to less-hindered isomer **11**, which can be captured by Grignard reagent to deliver the observed product after reductive elimination (and concomitant catalyst regeneration). Alternatively, **9** may undergo direct *anti*-attack by Grignard[27] to give η^2-complex **12**, which will again deliver the arylated spiroheterocyclic product, this time by decomplexation. Finally, it is possible that the process involves a radical mechanism[28]: if the initially formed σ-Fe–C bond undergoes homolysis to give aryl radical **13**, which cyclizes to give **14**, radical recombination will give the same η^1-intermediate **11** as postulated for the Fe(I)/(II) pathway. Since reactions carried out in the presence of radical inhibitors and scavengers had little discernable impact upon the yield of the reaction (reaction of **5-I** with $Fe(acac)_3$ and PhMgBr in the presence of 5 mol% of either TEMPO or BHT gave a 76% yield of **6a** in both cases), a radical chain pathway seems unlikely but the involvement of homolytic processes cannot be categorically excluded at this point.

In an attempt to gain insight into the nature of the iron catalyst involved in the reaction, we exposed $Fe(acac)_3$ to one equivalent of Grignard in the absence of iodide substrate; after careful manipulation of the product of this reaction we isolated and characterized bimetallic iron(II) complex **15**. When **15** was used in place of $Fe(acac)_3$ in the arylative spirocyclization reaction, a similar yield of product was obtained (Fig. 3), suggesting that this dearomatizing spirocyclization process proceeds through the intermediacy of an iron(II) species. Confirming the precise mechanistic details of the transformation is the subject of our research focus at this time.

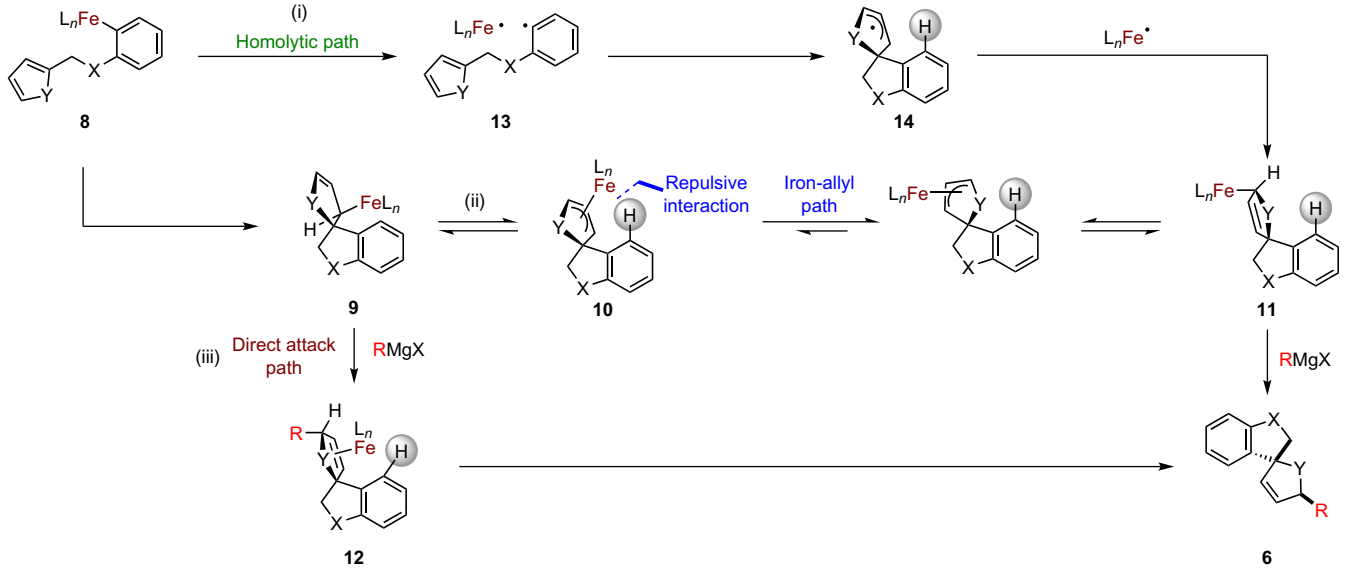

Figure 2 | Polar and free-radical mechanistic possibilities in iron-catalysed arylative spirocyclization. The mechanism by which the spirocyclization reaction proceeds could follow one of several routes: (i) Homolysis of the initial aryl-iron species **8** would lead, via ultimate radical recombination, to key π-allyl iron intermediate **11**; (ii) polar cyclization, followed by isomerization of η^2 π-allyl iron species **9** to intermediate **11** via **10**; or (iii) direct capture of η^2 π-allyl iron species **9** by a Grignard reagent.

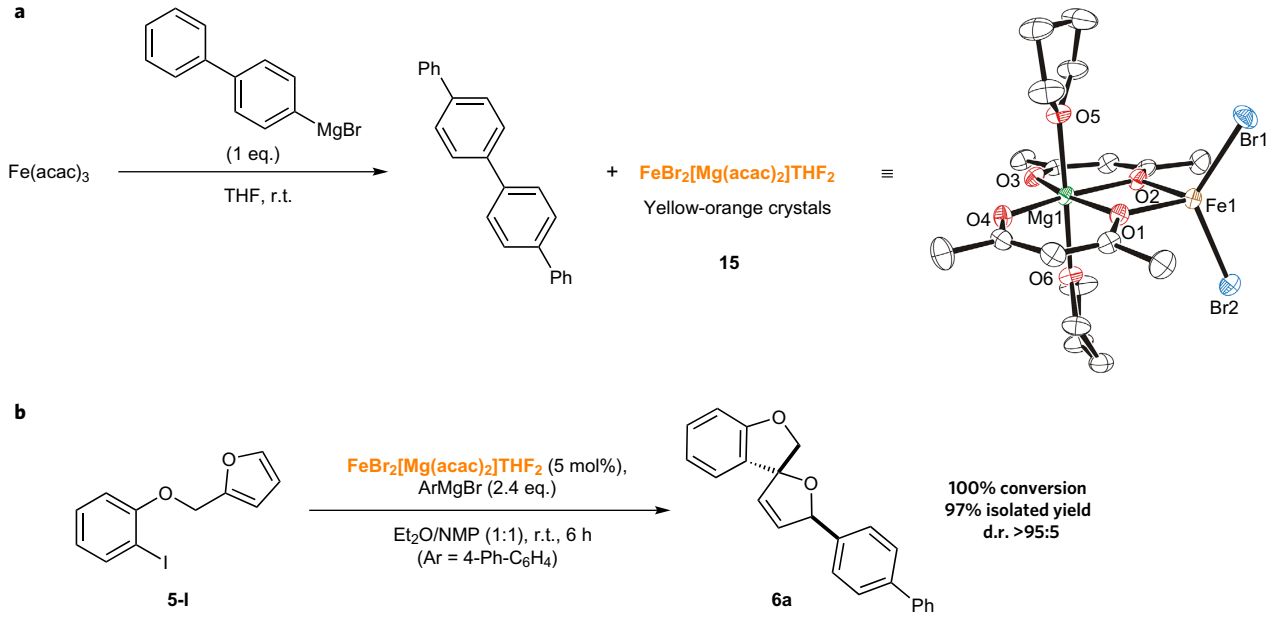

Figure 3 | Verification of the role of Fe(II) in the spirocyclization reaction. a, A bimetallic Mg–Fe(II) complex **15** is formed by the reaction of a Grignard reagent with the Fe(III) catalyst. This complex was isolated and characterized crystallographically. **b**, The Fe(II) product can catalyse the arylative spirocyclization reaction with comparable results to the reaction with $Fe(acac)_3$. While the precise mechanistic details of the reaction are still unknown, this suggests that an initial *in situ* reduction of the Fe(III) pre-catalyst is likely the first stage of the reaction, which may have implications in future developments of this reaction.

In summary, we have designed and implemented a novel cyclization/anion capture process, mediated by Earth-abundant catalysts, which efficiently delivers spiro-bisheterocycles. The process is efficient and rapidly delivers these complex frameworks in short order, using biomass-derived components.

Data availability

The crystallographic data have been deposited at the Cambridge Crystallographic Data Centre (CCDC) as CCDC 1508541 (**6c** at 150 K) and 1508540 (**15** at 150 K) and can be obtained free of charge from the CCDC via www.ccdc.cam.ac.uk/getstructures.

Received 1 April 2015; accepted 7 October 2016;
published online 12 December 2016

References

1. Kharasch, M. S. & Fields, E. K. Factors determining the course and mechanisms of Grignard reactions. IV. The effect of metallic halides on the reaction of aryl Grignard reagents and organic halides. *J. Am. Chem. Soc.* **63,** 2316–2320 (1941).
2. Tamura, M. & Kochi, J. Vinylation of Grignard reagents. Catalysis by iron. *J. Am. Chem. Soc.* **93,** 1487–1489 (1971).
3. Molander, G. A., Rahn, B. J., Shubert, D. C. & Bonde, S. E. Iron-catalyzed cross-coupling reactions. Synthesis of arylethenes. *Tetrahedron Lett.* **24,** 5449–5452 (1983).
4. Bolm, C., Legros, J., Le Paih, J. & Zani, L. Iron-catalyzed reactions in organic synthesis. *Chem. Rev.* **104,** 6217–6254 (2004).
5. Sherry, B. D. & Fürstner, A. The promise and challenge of iron-catalyzed cross-coupling. *Acc. Chem. Res.* **41,** 1500–1511 (2008).
6. Fürstner, A. From oblivion into the limelight: iron (domino) catalysis. *Angew. Chem. Int. Ed.* **48,** 1364–1367 (2009).
7. Bauer, I. & Knölker, H.-J. Iron catalysis in organic synthesis. *Chem. Rev.* **115,** 3170–3387 (2015).
8. Welsch, M. E., Snyder, S. A. & Stockwell, B. R. Privileged scaffolds for library design and drug discovery. *Curr. Opin. Chem. Biol.* **14,** 347–361 (2010).
9. Dal Piaz, F. *et al.* Identification and mechanism of action analysis of the new PARP-1 inhibitor 2″-hydroxygenkwanol A. *Biochim. Biophys. Acta* **1850,** 1806–1814 (2015).
10. Zhou, M. *et al.* Aspergillines A–E, highly oxygenated hexacyclic indole–tetrahydrofuran–tetramic acid derivatives from *Aspergillus versicolor*. *Org. Lett.* **16,** 5016–5019 (2014).
11. Franz, A. K., Dreyfuss, P. D. & Schreiber, S. L. Synthesis and cellular profiling of diverse organosilicon small molecules. *J. Am. Chem. Soc.* **129,** 1020–1021 (2007).
12. Hartwell, K. A. *et al.* Niche-based screening identifies small-molecule inhibitors of leukemia stem cells. *Nat. Chem. Biol.* **9,** 840–848 (2013).
13. Wu, J.-S., Zhang, X., Zhang, Y.-L. & Xie, J.-W. Synthesis and antifungal activities of novel polyheterocyclic spirooxindole derivatives. *Org. Biomol. Chem.* **13,** 4967–4975 (2015).
14. Badillo, J. J., Hanhan, N. V. & Franz, A. K. Enantioselective synthesis of substituted oxindoles and spirooxindoles with applications in drug discovery. *Curr. Opin. Drug Discov. Devel.* **13,** 758–776 (2010).
15. Zhuo, C.-X., Zheng, C. & You, S.-L. Transition-metal-catalyzed asymmetric allylic dearomatization reactions. *Acc. Chem. Res.* **47,** 2558–2573 (2014).
16. Adams, R. & Voorhees, V. Furfural. *Org. Synth.* **1,** 49–51 (1921).
17. Fürstner, A. *et al.* Preparation, structure, and reactivity of non-stabilized organoiron compounds. Implications for iron-catalyzed cross coupling reactions. *J. Am. Chem. Soc.* **130,** 8773–8787 (2008).
18. Cahiez, G. & Avedissian, H. Highly stereo- and chemoselective iron-catalyzed alkenylation of organomagnesium compounds. *Synthesis* 1199–1205 (1998).
19. Martín-Matute, B., Nevado, C., Cárdenas, D. J. & Echavarren, A. M. Intramolecular reactions of alkynes with furans and electron rich arenes catalyzed by $PtCl_2$: the role of platinum carbenes as intermediates. *J. Am. Chem. Soc.* **125,** 5757–5766 (2003).
20. Bedford, R. B. How low does iron go? Chasing the active species in Fe-catalyzed cross-coupling reactions. *Acc. Chem. Res.* **48,** 1485–1493 (2015).
21. Cassani, C., Bergonzini, G. & Wallentin, C.-J. Active species and mechanistic pathways in iron-catalyzed C–C bond-forming cross-coupling reactions. *ACS Catal.* **6,** 1640–1648 (2016).
22. Daifuku, S. L., Al-Afyouni, M. H., Snyder, B. E. R., Kneebone, J. L. & Neidig, M. L. A combined mössbauer, magnetic circular dichroism, and density functional theory approach for iron cross-coupling catalysis: electronic structure, in situ formation, and reactivity of iron-mesityl-bisphosphines. *J. Am. Chem. Soc.* **136,** 9132–9143 (2014).
23. Noda, D., Sunada, Y., Hatakeyama, T., Nakamura, M. & Nagashima, H. Effect of TMEDA on iron-catalyzed coupling reactions of ArMgX with alkyl halides. *J. Am. Chem. Soc.* **131,** 6078–6079 (2009).
24. Hatakeyama, T. *et al.* Iron-catalyzed suzuki–miyaura coupling of alkyl halides. *J. Am. Chem. Soc* **132,** 10674–10676 (2010).
25. Przyojski, J. A., Veggeberg, K. P., Arman, H. D. & Tonzetich, Z. J. Mechanistic studies of catalytic carbon–carbon cross-coupling by well-defined iron NHC complexes. *ACS Catal.* **5,** 5938–5946 (2015).

26. Krivykh, V. V., Gusev, O. V., Petrovskii, P. V. & Rybinskaya, M. I. Investigation of the stereochemistry of transition metal allyl cationic complexes. *J. Organomet. Chem.* **366,** 129–145 (1989).
27. Sekine, M., Ilies, L. & Nakamura, E. Iron-catalyzed allylic arylation of olefins via C(sp3)-H activation under mild conditions. *Org. Lett.* **15,** 714–717 (2013).
28. Ekomi, A. *et al*. Iron-catalyzed reductive radical cyclization of organic halides in the presence of $NaBH_4$: evidence of an active hydrido iron(I) catalyst. *Angew. Chem., Int. Ed.* **51,** 6942–6946 (2012).

Acknowledgements

The authors acknowledge financial support from the Engineering and Physical Sciences Research Council (Organic Synthesis Studentship grant EP/G040247/1), AstraZeneca Pharmaceuticals and the University of Huddersfield. J.B.S. is grateful to the Royal Society, for the award of an Industry Fellowship. Dedicated to the memory of Sarah Hicks, a young chemist who died at Hillsborough.

Author contributions

K.A., A.K.B., J.B., B.C., P.K.T.L. and J.R. carried out all cyclization experiments, under the supervision of J.B.S., aided by D.M.G. and P.R. Isolation of complex 15 was carried out by L.B. and J.B. under the supervision of N.J.P. and J.B.S. X-ray crystallography was carried out by C.R.R. The ideas were conceived by B.C. and J.B.S. Reactions were conceived and designed by J.B.S. The manuscript was written by J.B.S.

Additional information

Supplementary information and chemical compound information are available in the online version of the paper. Reprints and permissions information is available online at www.nature.com/reprints. Correspondence and requests for materials should be addressed to J.B.S.

Competing financial interests

The authors declare no competing financial interests.